Vol. 29: 41–52, 2005 | CLIMATE RESEARCH Clim Res | Published July 20

# Probabilistic distributions of regional climate change and their application in risk analysis of wheat production

**Qunying Luo[1,*], Roger N. Jones[2], Martin Williams[1], Brett Bryan[3], William Bellotti[4]**

[1]Department of Geographical and Environmental Studies, University of Adelaide, North Terrace, Adelaide, South Australia 5005, Australia

[2]Climate Impact Group, CSIRO Atmospheric Research, Private Bag 1, Aspendale, Victoria 3195, Australia

[3]Policy and Economic Research Unit, CSIRO Land and Water, Private Bag 2, Glen Osmond, South Australia 5064, Australia

[4]School of Agriculture & Wine, University of Adelaide, South Australia 5371, Australia

ABSTRACT: Downscaled outputs from 9 climate models and information from the 2000 Intergovernmental Panel on Climate Change (IPCC) Special Report on Emission Scenarios (SRES) were used to construct probability distributions of regional climate change for Roseworthy, South Australia. The construction of probability distribution for regional climate change involved the identification, quantification and treatment of uncertainties from greenhouse gas (GHG) emission scenarios, climate sensitivity and local climate change. Monte Carlo random sampling techniques were applied to component ranges of uncertainty defined by quantified upper and lower limits, assuming uniform probability over each range. Construction of resulting probability distributions of regional climate provided a framework for risk analysis. These probabilities were applied to the Agricultural Production System sIMulator (APSIM)-Wheat model to evaluate potential wheat production at Roseworthy for the year 2080 through the identification of critical yield thresholds. The conditional probability of not meeting the critical yield threshold increased from 27% under baseline conditions to 45% under the median probability for the year 2080, indicating less profitable wheat production in the study area.

KEY WORDS: Probability distribution functions · Monte Carlo random sampling · Uncertainty management · Climate change · APSIM-Wheat model · Risk analysis · Wheat production



## 1. INTRODUCTION

Accelerating levels of greenhouse gas (GHG) emissions ($CO_2$, $N_2O$, $CH_4$) arising from human activities such as fossil fuel burning, land use change, biomass burning and cement production are considered actual and potential agents of climatic change (Prentice et al. 2001). Changes in the concentration of atmospheric $CO_2$ ($pCO_2$) and consequent climate changes have significant implications for natural ecosystems and for human society at scales ranging from local to regional and global. Construction of climate change scenarios is one of the key steps in assessing the potential impacts on many activities, including wheat production. Scenarios based on general circulation models (GCMs) are the most common type used in impact assessment (Mearns et al. 2001). Most impact studies have applied single scenarios or several scenarios derived from different GCMs presented as alternative outcomes. This approach provides first-order impacts of climate change such as crop yield and grain protein content.

Large differences in both the global and regional output of different GCMs and RCMs (regional circulation models) reflect the underlying uncertainties, making it difficult for scientists to judge model accuracy in predicting climate change. Faced with this dilemma, it is prudent to apply a range of model-generated scenarios to explore the possible impacts. Assessment results

*Email: qunying.luo@adelaide.edu.au

derived from single scenarios appear precise, but are conditional to those particular scenarios. Such results are unlikely to represent other possible futures as the results were not based on the full spectrum of future climate change scenarios and thus are highly speculative (Hulme & Carter 1999). Outcomes based on single scenarios, or even on a range of scenarios, are plausible, but contain no information as to their likelihood. While appropriate for testing sensitivity and the vulnerability of a particular system, the use of plausible climate change scenarios without investigating likelihood is poorly suited for planning or policy purposes (Jones 2000a, Ahmad et al. 2001).

Numerous uncertainties exist at every step of climate change impact assessment, from the projections of GHG emissions to projections of global and of regional climate change. All 3 sources of uncertainty propagate through impact assessments (Henderson-Sellers 1993, Ahmad et al. 2001). It is therefore urgent that uncertainties surrounding impact assessment be identified and quantified, so that the results can be used for policy making and for devising future adaptation strategies. Uncertainty analysis can provide an estimate of confidence limits on model results and would be of value in the application of these results in risk and policy analyses (Leavesley 1994).

The quantification and treatment of uncertainty associated with the projection of global warming have been analysed in far greater detail than is the case for impact assessment. Two principal methods have been used to attach probabilities to impacts: (1) application of a large number of scenarios to an impact assessment and creation of a probability distribution from the outcomes; (2) creation of an underlying probability distribution for each successive stage of analysis, explicitly managing the underlying uncertainty at each stage. Titus & Narayan (1996) and Yohe & Schlesinger (1998) provide examples of the first method; both studies illustrate the probabilities of sea level rise and consequent impacts.

The second method, which we use in this study, is described by Hulme & Carter (1999) and Jones (2000b). The latter author identified, quantified and treated uncertainties associated with global warming and local climate change for assessing the possible impacts of climate change on irrigation water demand. Similar approaches have been used to assess changes in water resources at the catchment scale (Jones & Page 2001) and on milk production (Jones & Hennessy 2000). Howden et al. (1999) evaluated the possible impacts of climate change on wheat grain yield and grain nitrogen content with atmospheric $pCO_2$ fixed at 700 ppm, and Howden & Jones (2001) undertook a probabilistic analysis of the costs and benefits of climate change on Australia's national wheat crop.

Atmospheric $pCO_2$ has a critical influence on plant growth, thus affecting wheat production. Increasing $pCO_2$ is likely to enhance crop production through the stimulation of photosynthesis and improvement of water use efficiency. Hence, uncertainties related to atmospheric $pCO_2$ change also need to be identified, quantified and treated. The Intergovernmental Panel on Climate Change (IPCC) Special Report on Emission Scenarios (SRES) (Nakiçenovic et al. 2000) provides projections of change in atmospheric $pCO_2$ to 2100 (Prentice et al. 2001), which is a prerequisite for evaluating uncertainty in biological systems. The methodological problems noted above motivated our reassessment of impacts on wheat production. The SRES imply a warmer climate than the earlier IS92a-f scenarios, and this has significant implications for agriculture.

In this study, we constructed probability distribution functions for the year 2080 through the identification, quantification and treatment of uncertainties associated with regional climate change projection, and we used them to analyse risk (higher-order economic effects) in a wheat production system. Section 2 deals with identification, quantification and treatment of uncertainties associated with the construction of regional climate change scenarios. Section 3 describes the application of constructed probability distributions to risk analysis in a wheat production system in South Australia.

## 2. CONSTRUCTION OF CLIMATE CHANGE SCENARIOS

### 2.1. Identification of uncertainties

'Uncertainty' can be applied to any notion from confidence just short of certainty to informed guesses or speculation. Lack of information obviously results in uncertainty, but often disagreement about what is known, or even knowable, is also a source of uncertainty (Ahmad et al. 2001). There are many sources of uncertainty associated with GHG emission projections, climate sensitivity, and local climate change projections. Some categories of uncertainty are amenable to quantification, while others cannot be expressed sensibly in terms of probabilities. Table 1 summarises the sources of uncertainty in projecting GHG and aerosol emissions, climate sensitivity, and regional climate response. GHG emissions are subject to uncertainties concerning population growth, technological change, and social and political behaviour. Climate model responses are most uncertain in how they represent feedback effects, particularly those dealing with changes to cloud regimes, biological effects, and ocean–atmosphere interactions. The coarse spatial resolution of climate models limits

Table 1. Uncertainties associated with the derivation of regional climate change. GHG: greenhouse gas

| Type of uncertainty | Source of uncertainty | Expression | Source |
|---|---|---|---|
| Greenhouse gas emissions | Social, economic, physical (accounting) | Mass or volume per year | Pepper et al. (1992)[a], Nakiçenovic et al. (2000)[b] |
| Aerosol emissions | Social, physical (accounting), economic | Mass or volume per year | IPCC (2001)[b] |
| Climate sensitivity | Scientific, emergent chaotic behaviour | Global warming for a $2 \times CO_2$ atmosphere, or per unit of GHG forcing | IPCC (2001), Hansen et al. (1998) |
| Regional climate response | Scientific, emergent chaotic behaviour | Local change per °C of global warming | CSIRO (2001), Page & Jones (2001)[c] |

[a]IPCC IS92a-f; [b]SRES; [c]OzClim

their ability to simulate regional climate change (CSIRO 2001). In Table 1, uncertainties from projections of GHG emissions, aerosol emissions and climate sensitivity contribute to uncertainties in estimating the degree of global warming. Regional climate response affects the calculation of local climate change, which is derived from a number of GCMs, and measured as local climate change per °C of global warming.

### 2.2. Quantification of uncertainties

Uncertainties about the impact of future human behaviour on GHG emissions and shortcomings in climate modelling limit climate projections to ranges of change for some variables, and to qualified statements on possible changes for others. Uncertainties have been quantified where possible with regard to future GHG emissions, climate sensitivity, and differences between models in simulating both global and regional climate responses. The method applied here is to use quantified scenarios to derive ranges of change for a selection of climate change uncertainties.

#### 2.2.1. Projections of atmospheric $pCO_2$ and climate sensitivity

Projections of global warming in our study range from 1990 to 2100 (Cubasch et al. 2001), on the basis of SRES with an updated version of the simple climate model (Model for the Assessment of Greenhouse-gas Induced Climate Change, MAGICC; Wigley 2003) that was used in the construction of the IPCC (1996) projections of global warming. These projections deal with the first 3 types of uncertainty listed in Table 1. The main difference between the 2 sets of projected global warming is due to the replacement of the IS92a-f scenarios with those from the SRES.

The SRES assume that there will be no specific GHG mitigation activities (Nakiçenovic et al. 2000). The scenarios are based on a range of assumptions about population, energy sources, and regional or global approaches to development and socio-economic arrangements; these are updates of the IS92a-f scenarios. In SRES, sulphate aerosol emissions (which have a cooling effect) are projected to undergo greater reductions than in the IS92a-f scenarios, particularly after 2050 (Nakiçenovic et al. 2000). Thus, the projected range of warming in 2100 is greater than that expected by IPCC (1996).

Nakiçenovic et al. (2000) developed 4 narrative storylines for the 21st century (A1, A2, B1, and B2). Each storyline represents different demographic, social, economic, technological, and environmental developments. Storyline A1 and its associated scenarios describe a future world with very rapid economic growth, a global population peak at mid-century and subsequent decline, and rapid introduction of new and more efficient technologies. The A1 scenario family develops into 3 groups with different directions of energy technology: fossil intensive (A1F), non-fossil energy sources (A1T), or a balance across all sources (A1B). Storyline A2 assumes a very heterogeneous world. The underlying theme is self-reliance and preservation of local identities. Storyline B1 describes a convergent world with the same global population as Storyline A1, but with rapid change in economic structures toward a service and information economy, with reductions in material intensity and the introduction of clean and resource-efficient technologies. Storyline B2 and its scenario family describes a world in which the emphasis is on local solutions to economic, social and environmental sustainability (Nakiçenovic et al. 2000). No preference was given to any of the scenarios and they were not assigned probabilities of occurrence. Model studies were then used to quantify the relationship between the storylines and emissions. Table 2

Table 2. Scenarios used in this study for atmospheric $pCO_2$ and greenhouse gas (GHG) forcing from 1990 to 2080. Data from IPCC Data Distribution Center (available at: http://ipcc-ddc.cru.uea.ac.uk). **Bold:** upper and lower ends for atmospheric $pCO_2$

| Model | $pCO_2$ (ppm) | GHG forcing (W $m^{-2}$) |
|---|---|---|
| A1B | 639 | 5.62 |
| A1T | 563 | 5.11 |
| A1F | **786** | 7.89 |
| A2 | 682 | 6.4 |
| B1 | **530** | 4.09 |
| B2 | 552 | 4.92 |

gives quantified uncertainties for atmospheric $pCO_2$ and GHG forcing for the year 2080 under the 6 marker scenarios of the SRES (A1B, A1T, A1F, A2, B1 and B2). Table 3 shows the quantified uncertainty of climate sensitivity from 7 GCMs used in projecting global warming under the 6 emission scenarios. The bold values in these 2 tables are upper and lower ends for atmospheric $pCO_2$ and λ (a factor associated with climate sensitivity), which were used in the Monte Carlo random sampling procedures (Section 2.3).

### 2.2.2. Projections of GHG and sulphate aerosol forcing, and of global warming

Probability distributions for global warming were produced from 2 factors: (1) GHG and sulphate aerosol forcing, and (2) climate sensitivity. The latter is represented by the factor λ which was multiplied with radiative forcing, using a method similar to that applied by Schneider (2001). GHG forcing is closely related to atmospheric $pCO_2$ as shown in Eq. (1) and Fig. 1, which

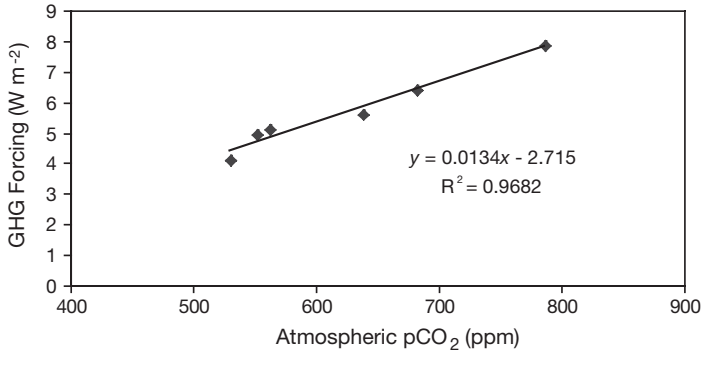


Fig. 1. Relationship between greenhouse gas (GHG) forcing and atmospheric $pCO_2$. The standard error is 0.77 for the intercept and $10^{-3}$ for the gradient. Both the intercept and gradient are significantly related to the dependent variable GHG forcing at a 0.05 significance level (p = 0.02 for the intercept and $4 \times 10^{-4}$ for the gradient)

Table 3. Average climate sensitivities λ of 7 global climate models. **Bold:** upper and lower ends for λ

| Model | λ (°C $m^2$ $W^{-1}$) |
|---|---|
| GFDL | **0.568** |
| CSIRO | 0.530 |
| HADCM3 | 0.529 |
| HADCM2 | 0.458 |
| ECHAM4 | 0.386 |
| CSM | 0.368 |
| PCM | **0.326** |

was obtained by using information on GHG and aerosol forcing and on atmospheric $pCO_2$ under the 6 marker scenarios of the SRES (Table 2). The differences can be explained by different relative levels of non-$CO_2$ GHGs, sulphate aerosols and land cover in the 6 scenarios. The standard error is very small for both intercept (0.77) and gradient (0.001) of Eq. (1). The intercept and gradient of Eq. (1) are significantly related to the dependent variable, GHG forcing, with p values $<0.05$. Projection of global warming is based on Eq. (2) (Chapter 15 in Brasseur et al. 1999).

$$\text{GHG forcing} = 0.0134 \times pCO_2 - 2.715 \quad (1)$$

$$\text{Global temperature change} = \text{GHG forcing} \times \lambda \quad (2)$$

where λ is a GCM specific factor; 'GHG forcing' here accounts for both GHGs and sulphate aerosols. We took this approach in order to relate $pCO_2$, radiative forcing and climate sensitivity within a probabilistic framework. As can be seen by the close relationship between $pCO_2$ and radiative forcing for the 6 SRES marker scenarios, this approximation of the complex relationship will create only small variations in the possible outcomes.

### 2.2.3. Projections of local climate change

This study is focused on the town of Roseworthy, situated in the heart of a major wheat production region in South Australia (Fig. 2). There are significant differences between models with regard to climatic changes simulated at the regional scale (from 10 to 50 km, to subcontinental), particularly in the case of precipitation. Thus, in order to represent this uncertainty, output from a range of climate models was used to construct probabilistic distributions of local climate change.

Ranges of uncertainty in local climate were assembled using OzClim (Page & Jones 2001), a grid-based regional climate change scenario generator. Anomalies of local change in temperature and rainfall for each month at each model grid point of a range of GCMs/RCMs have been linearly regressed against

Table 4. Overview of the 9 global and regional circulation models (GCMs and RCMs) used in this study

| Model | Institution | Emission scenarios | Years | Spatial resolution (km) | Temporal resolution |
|---|---|---|---|---|---|
| MK2 | CSIRO, Australia | IS92a, SRES A2[a], SRES B2 | 1881–2100[b] | ≈ 400 | Daily |
| CGCM1 | Canadian CCCM | 1% $yr^{-1}$ increase in $CO_2$ | 1900–2100 | ≈ 400 | Monthly |
| GFDL-R15-a | GFDL, USA | 1% $yr^{-1}$ increase in $CO_2$ | 1958–2057 | ≈ 500 | Monthly |
| HADCM2 | Hadley Center, UK | 1% $yr^{-1}$ increase in $CO_2$[a] | 1860–2100 | ≈ 400 | Monthly |
| HADCM3 | Hadley Center, UK | IS92a | 1861–2099 | ≈ 400 | Monthly |
| ECHM3/LSG | DKRZ, Germany | IS92a | 1880–2085 | ≈ 600 | Monthly |
| ECHM4/OPYC3 | DKRZ, Germany | IS92a | 1860–2099 | ≈ 300 | Monthly |
| DARLAM | CSIRO, Australia | Nested in MK2 with IS92a | 1961–2100 | ≈ 125 | Daily |
| NCAR DOE-PCM | NCAR, USA | IS92a | 1960–2099 | ≈ 500 | Monthly |

[a]4 simulations; [b]pre-1990 period common to the SRES simulations

annual average global warming over the transient run to produce a measure of local change per °C of global warming. These patterns of local monthly climate change information were linearly interpolated onto a 0.5° geographical grid for Australia and incorporated into OzClim, making them available for scaling under different assumptions of climate sensitivity and GHG emissions (Page & Jones 2001); see Table 4 for an overview of the 9 models used. The models were obtained from CSIRO and the IPCC Data Distribution Centre (http://ipcc-ddc.cru.uea.ac.uk). Quality control and methods for calculating regional climate change are summarised in Whetton (2001) (www.dar.csiro.au/impacts/docs/how.pdf). The models in Table 4 are grid-based coupled atmosphere–ocean GCMs with 1 RCM nested in a coupled GCM. Most of them reproduce the observed 1961 to 1990 climatology of rainfall and temperature quite well in the South Australia region (McInnes 2002). They comprise a set of GCMs similar to that used to calculate the range of global warming in Cubasch et al. (2001), with the omission of 1 poorly performing global model and the addition of a regional climate model.

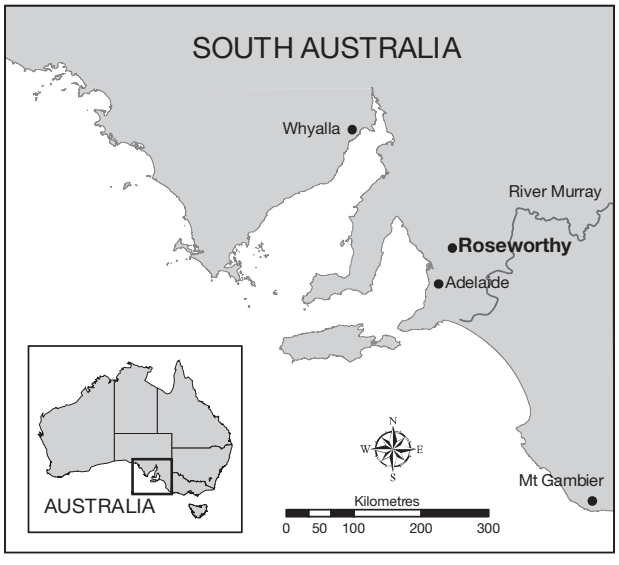


Fig. 2. Study location in South Australia

### 2.3. Treatment of uncertainties

The Monte Carlo random sampling (MCRS) technique was applied to develop probability distribution functions (PDFs) of regional climate change. MCRS is the best-known method for propagating probability distributions of parameters to determine the probability distributions of outcomes. In this case, ranges of change for radiative change, climate model sensitivity, $pCO_2$ and local climate change centred on Roseworthy were combined and used to calculate the risks that climate change may pose to wheat yield. The method used created ranges of change for each of the input variables, assumed a prior distribution for each of those ranges, sampled within each of the ranges and combined the inputs in a manner consistent with the application of single scenarios, i.e. by maintaining levels of (in)dependence where appropriate.

#### 2.3.1. Construction of ranges for local climate change, atmospheric $pCO_2$ and λ

Construction of the range of values for each independent variable is the first step in the MCRS technique. Atmospheric $pCO_2$, λ (climate sensitivity) and local climate change, measured as a function of global warming, were randomly sampled as independent variables. Resultant ranges of radiative forcing and global warming were dependent on those variables. The ranges for local temperature and local rainfall per

°C of global warming incorporate quantifiable uncertainties among the 9 climate models. For temperature change at Roseworthy, the average annual change was calculated (Table 5). For rainfall, the monthly rainfall change was averaged according to growing season (GS: May to October inclusive) and non-growing season (NGS: November to April inclusive) for each of the 9 climate models. Differential weighting was applied to each month based on the ratio of rainfall in that month to annual rainfall. The averaged results (Table 5) were used to extract ranges for the GS and NGS season rainfall change. The ranges for all independent variables (local rainfall and temperature change, atmospheric $pCO_2$ and λ) are listed in Table 6 and show that rainfall is projected to decrease in both GS and NGS.

### 2.3.2. Monte Carlo random sampling

Construction of the ranges for local temperature, GS and NGS rainfall, atmospheric $pCO_2$, and λ allowed Monte Carlo sampling to commence. Several assumptions were made concerning the prior distribution of data ranges and the sampling procedures. Each of the above ranges was assumed to have a uniform probability of occurrence following the method outlined in Jones (2000b). This is a very conservative assumption that gives the individual samples no probability, save for the highest and lowest estimate constraining the range. However, by combining several ranges of uncertainty in this manner, the product is non-uniform due to the central limit theorem of classical statistics (Jones 2000a, Wigley & Raper 2001). Thus, the assumption is that the contributing scenarios have no intrinsic likelihood beyond being plausible. For $pCO_2$, this assumes that although the SRES process developed 4 future storylines which were used to quantify $pCO_2$, those outcomes are no more likely than possibilities encompassed within the range that were not identified. The range produced by the SRES process also encompasses most of the range covered by pre-existing scenarios (Nakiçenovic et al. 2000), so that it is representative of plausible outcomes in an environment where large GHG reductions or stabilisation do not occur. λ has recently been the subject of a series of studies providing PDFs for climate model sensitivity (see Dessai & Hulme 2004). However, these non-linearities have not been represented here. Regional change in both rainfall and temperature are assumed to be uniform across the range of outcomes, despite recent efforts to provide PDFs for multiple models (e.g. Giorgi & Mearns 2003). There are no noticeable correlations between local rainfall change and temperature change in Australia.

Ranges for atmospheric $pCO_2$, λ and local temperature were assumed to have a uniform distribution and were randomly sampled 100 000 times based on the ranges given in Table 6 (Fig. 3a,b,d). Large samples of GHG forcing and global warming were derived from Eqs. (1) & (2), respectively (see Section 2.2.2). The distribution of global warming is non-uniform, peaking around an average value (Fig. 3c). This non-linear distribution for global warming also contributes to non-linear PDFs for local temperature and rainfall change. Regional temperature is calculated as the multiplication of global temperature and local temperature (per °C of global warming) and its distribution is shown in Fig. 3e: a non-uniform distribution, but more skewed than that of global warming. Local rainfall change was divided into separate ranges for GS and NGS, expressed as a percentage change per °C of global warming (Table 6). Global warming was used to scale the possible ranges for GS and NGS rainfall change. The lower and upper limits for GS and NGS rainfall change were multiplied by the upper limit for global warming (i.e. 4.43°C) to ensure that values anomalous to that degree of warming were not sampled. In other words, the upper and lower limits of rainfall change in GS and NGS were constrained by the upper limit of global warming to derive all possible outcomes of regional rainfall

Table 5. Local climate change from 1990 to 2080 at Roseworthy, South Australia, according to each of the models described in Table 4. GS: growing season; NGS: non-growing season. **Bold:** upper and lower ends for local temperature, local GS and NGS rainfall changes

| Model | Temperature (change in °C) | Rainfall (change in %) GS | NGS |
|---|---|---|---|
| MK2 | 0.95 | **–7.35** | –3.44 |
| CGCM1 | **0.77** | –4.28 | –0.93 |
| R15-a | **1.08** | **2.76** | –3.65 |
| HADCM2 | 0.88 | –3.58 | **–6.74** |
| HADCM3 | 0.99 | –6.81 | –5.67 |
| OPYC3 | 0.82 | –6.45 | –2.63 |
| LSG | 1.03 | –6.03 | **11.11** |
| DARLAM | 0.83 | –2.82 | 3.60 |
| DOE-PCM | 0.93 | –2.74 | –2.49 |

Table 6. Ranges for local climate change, atmospheric $pCO_2$, and λ from 1990 to 2080 at Roseworthy, South Australia. GS: growing season; NGS: non-growing season

| Temperature (change in °C) | Rainfall (change in %) GS | NGS | $pCO_2$ (ppm) | λ |
|---|---|---|---|---|
| 0.77 to 1.08 | –7.35 to 2.76 | –6.74 to 11.11 | 530 to 786 | 0.326 to 0.568 |

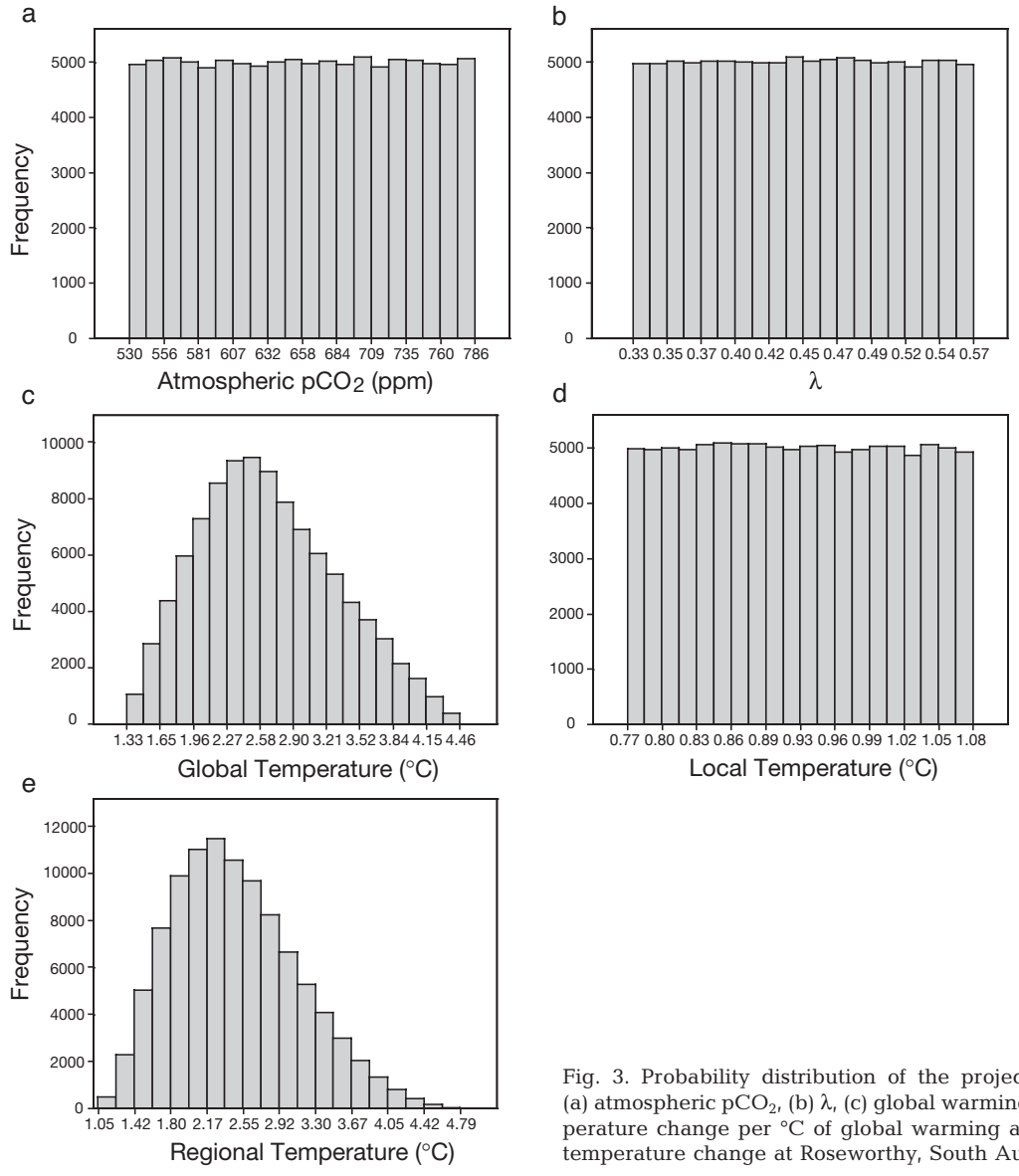


Fig. 3. Probability distribution of the projected ranges for (a) atmospheric $pCO_2$, (b) λ, (c) global warming, (d) local temperature change per °C of global warming and (e) regional temperature change at Roseworthy, South Australia, in 2080

for these 2 seasons. The 2 amended ranges were then sampled separately 100 000 times. Samples from these 2 ranges were then averaged to obtain regional rainfall change with a weighting of ⅔ given to GS rainfall change and ⅓ given to NGS rainfall change. The weighting is based on the distribution of rainfall during GS and NGS under the current climate. Autocorrelation between rainfall amounts in GS and NGS was not considered.

### 2.3.3. Generation of probabilistic scenarios

The random samples of climate change scenarios for regional temperature, regional rainfall and $CO_2$ change were grouped into classes and summarised. Class breaks were created at every 5% change in $CO_2$ and rainfall and 0.5°C change in temperature. A distinct climate change scenario class was created for unique combinations of $CO_2$, rainfall and temperature change class breaks. Each randomly sampled scenario was allocated to the nearest class and the total count of scenarios occurring in each class was tabulated. The probability for each class was calculated by dividing the number of randomly sampled scenarios in the class by the total number of scenarios (100 000). Scenario classes were then ranked from the most likely to the least likely. The cumulative probability was calculated by summing probabilities from the most likely to the least likely scenario class.

The cumulative probabilities of each scenario class were used to create 3 bivariate contour graphs ($CO_2$ vs.

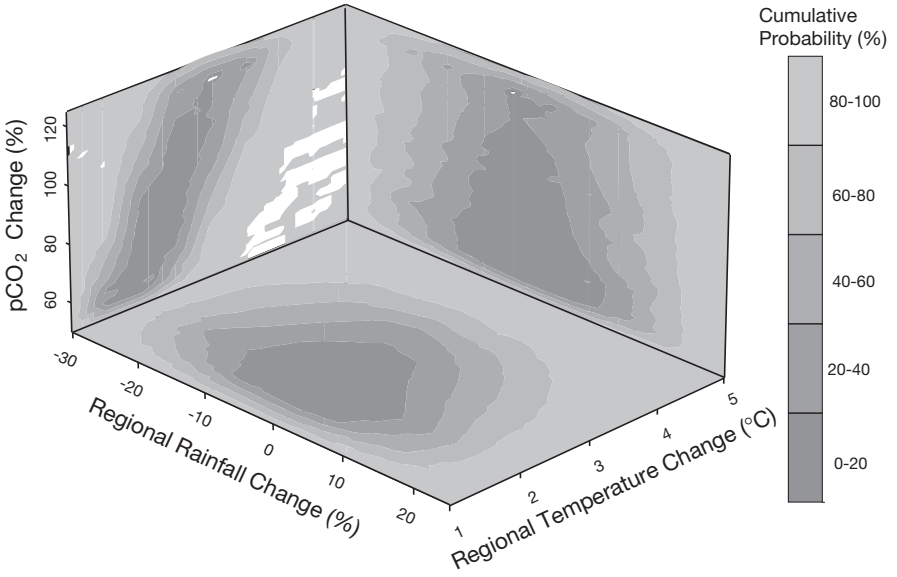


Fig. 4. Probabilistic climate change scenarios for Roseworthy, South Australia, in 2080. Shaded areas represent the cumulative probability of certain levels of rainfall, temperature and $pCO_2$. The darkest shade represents the most likely climate change scenarios with a cumulative probability ranging from 0 to 20%. The lightest shade stands for the least likely climate change scenario with a cumulative probability between 80 and 100%

rainfall, rainfall vs. temperature, temperature vs. $CO_2$). Each graph displays the likelihood of occurrence of difference climate change scenarios. We defined 5 contour classes visualised by different shades of grey for each graph, representing cumulative probability quintiles such that each contour class contains 20% of the total number of random samples (cf. Fig. 3). The darkest shade of grey represents the 20% most likely climate change scenarios, and the lightest shade represents the 20% least likely scenarios. Each bivariate graph (Fig. 4) is essentially a projection of the volume onto the graph wall. For example, the bivariate graph of rainfall vs. temperature represents probabilities for all values of $CO_2$, rather than a slice of those probabilities occurring at the planar intersection of the chart in the diagram. The projected range with a low probability of occurrence (≤20%) occupies a larger portion of space. This means that a large uncertainty created by combining results from different GCMs/RCMs and SRES can potentially be treated through statistical techniques. There are some blank patches in the plotting area due to the incorporation of the relationship between atmospheric $pCO_2$ and regional temperature: regional temperature = local temperature × λ × $(0.0134 \times pCO_2 - 2.715)$.

## 3. PROBABILISTIC SCENARIOS IN RISK ANALYSIS

Risk analysis has emerged recently in the field of climate change impact assessment and focuses on the treatment of quantified uncertainties. Rather than being the end result, levels of performance relating to a specific impact can be addressed in the initial stages of risk assessment. These levels of performance then become the criteria against which risk can be evaluated in the light of system uncertainties. In the context of climate change impacts, these criteria are referred to as thresholds—the point where a stimulus leads to a significant response (Parry et al. 1996). The aim of risk analysis is to quantify the relationship between impact thresholds and the uncertainty space created from the combination of key environmental variables under climate change (Jones 2001). If the uncertainties surrounding projected climate change and its effect on particular impacts can be treated, then the probability of threshold exceedance/non-exceedance can be calculated and the consequences (i.e. risk) can be assessed. Risk analysis utilising projected ranges of uncertainties can be used to determine the conditional probability of exceeding/not exceeding the critical impact threshold. The PDFs produced above were applied to the Agricultural Production System sIMulator (APSIM)-Wheat model to analyse the possible risks of climate change to wheat production in Roseworthy.

### 3.1. APSIM-Wheat model

The APSIM-Wheat model is an integration of several interactive modules including biological modules (crop modules, soil module, etc.), and other utility and application modules. The wheat module is one of the crop modules within the APSIM system. It simulates the growth and development of a wheat crop in daily timesteps on an area basis as a function of weather (temperature, rainfall and solar radiation), soil (soil water and soil nitrogen), crop genetic coefficients and crop

Table 7. Cultivar genetic coefficients used by the APSIM-Wheat model (data from Yunusa et al. 2004)

| Coefficient | Janz | Excalibur |
|---|---|---|
| Sensitivity to vernalisation | 1.0 | 1.5 |
| Sensitivity to daylength | 2.0 | 2.0 |
| Grain filling duration (°C × d) | 640 | 703 |
| Grain number per head | 34.0 | 27.0 |
| Rate of grain filling (mg $d^{-1}$) | 2.5 | 3.5 |
| Stem weight (mg) | 1.65 | 2.4 |
| Phyllochron interval (°C × d) | 95 | 95 |
| Specific leaf area (mg $cm^{-2}$) | 185 | 180 |

Table 8. Levels of change (%) in rainfall used in the APSIM-Wheat model. GS: growing season; NGS: non-growing season

| Level | Rainfall GS | Rainfall NGS | Regional temp. (°C) | Atmospheric $pCO_2$ (ppm) |
|---|---|---|---|---|
| 1 | −28.58 | −26.89 | 1 | 527.2 |
| 2 | −28.36 | 9.97 | 2 | 634.8 |
| 3 | −12.32 | 16.23 | 3 | 687.4 |
| 4 | −3.50 | 32.31 | 4 | 785.8 |
| 5 | 10.83 | 46.28 | | |

Table 9. Factors considered in calculating the critical yield threshold. Prices are Australian $

| Variable | Value |
|---|---|
| Farm size (ha) | 500 |
| Grain price ($ $ha^{-1}$) | 170 |
| Interest rate (% $yr^{-1}$) | 10 |
| Labour hours (h $ha^{-1}$) | 1.2 |
| Labour price ($ $h^{-1}$) | 11 |
| Value of machinery ($) | 100 000 |
| Rate of depreciation of machinery (% $yr^{-1}$) | 16 |
| Allowance for other overheads ($) | 5000 |
| Land value ($ $ha^{-1}$) | 2000 |
| Long-term average return on agricultural land (% $yr^{-1}$) | 3 |
| Critical yield threshold (t $ha^{-1}$) | 1.87 |

management information (Keating et al. 2003, Luo 2003). The model has been tested in South Australia using simulating baseline grain yield (assuming current agricultural technology and management regimes) and historical wheat yields across 6 wheat production areas ($r^2$ = 0.92; Luo 2003).

Historical daily climate data for 1900 to 1999 were used to represent baseline climate. Two types of wheat cultivar (Janz and Excalibur) were represented in this study (Table 7). Soil nitrogen, soil water, and residues were reset on 1 March for each year of simulation run. The sowing rule was specified as follows: if cumulative rainfall ≥20 mm occurs within 3 d between 15 April and 15 June, then sow Janz; if cumulative rainfall ≥15 mm occurs within 3 d between 15 June and 15 August, then sow Excalibur. The model has the ability to constrain sowing time to once per year. If neither of these conditions was fulfilled, no crop was sown and the corresponding yield was zero. Sowing density was 200 plants $m^{-2}$, at a depth of 3 cm. Fertiliser application was 40 kg $ha^{-1}$ $NO_3$-N at planting date at a depth of 5 cm. In addition, initial soil $NO_3$-N was set at 60 kg $ha^{-1}$ in the top 35 cm of the soil profile. These levels were chosen to represent a non-limiting nitrogen environment.

We chose 5 rainfall, 4 temperature and 4 $CO_2$ concentration levels (Table 8) from the distribution illustrated in Fig. 4 to perturb the historical 100 yr daily climate data for the site under study, producing a total of 81 simulation runs: 80 climate change scenarios (5 × 4 × 4) and 1 baseline. Solar radiation was held constant.

### 3.2. Risk analysis

Risk is defined here as the conditional probability of not exceeding a critical yield threshold. Higher conditional probability means higher risk to wheat production. For example, if the conditional probability is 60% in a particular location, wheat yield will be poor in 6 of every 10 yr. A conditional probability of exceeding the critical yield threshold in ≥50% of the years is regarded as non-viable for farm economy in this study.

The critical yield threshold was identified through the cost–benefit analysis of farm profit. The calculation of profit involves many factors (Table 9). Some of these variables, such as land value and machine value, are depend on annual rainfall. The long-term average return on agricultural land is set at ≥3%. Once the other factors have been determined, production must exceed a critical yield corresponding to a 3% return, below which the wheat industry is not sustainable. Eqs. (a) to (g) in Table 10 were used to derive a critical yield threshold combined with the information provided in Table 9. The critical yield threshold can be derived by substituting Eqs. (c) to (g) into Eq. (b) and by substituting Eq. (b) into Eq. (a). The critical wheat yield for Roseworthy was 1.87 t $ha^{-1}$. If prevailing economic conditions become different from those assumed in this study, it is a relatively simple procedure to modify the model's assumptions.

The probability of not meeting the critical yield was calculated using the 100 yr simulation runs for each of the 80 climate change scenarios. The results are depicted in a risk response surface (lines in Fig. 5), superimposing the probabilistic climate change scenarios (shaded area).

The conditional probability of not meeting the critical yield threshold in 2080 ranges from 17 to 76%, compared to a current risk level of 27%, depending on the levels of change. Under the median level of climate change the conditional probability increases to 45% (medium risk level). To maintain current levels of productivity under these conditions would require implementing adaptive strategies and agricultural management measures such as adjusting sowing dates, cultivars, and fertiliser application, plant breeding and use of seasonal forecasts.

Table 10. Equations used to derive critical yield threshold

$$LTAR = NM/RLCM = 3\% \quad (a)$$

where LTAR is long-term average return on agricultural land (3%), NM is the net margin, and RLCM is the return on land capital and management-land value

$$NM = GM - IN - APFL - AMO - AOO \quad (b)$$

where GM is the gross margin, IN is the interest, APFL is the allowance for permanent and family labor, AMO is the allowance for machinery overheads, and AOO is the allowance for other overheads

$$GM = CY \times YP - VE \quad (c)$$

where CY is the critical yield, YP is the yield price, and VE is the variable expense

$$IN = \text{interest rate} \times VE/2 \quad (d)$$

$$APFL = \text{labor hour} \times \text{labor price} \quad (e)$$

$$AMO = \text{value of machinery} \times \text{depreciation rate/farm size} \quad (f)$$

$$AOO = \text{total overheads/farm size} \quad (g)$$

## 4. DISCUSSION

This study demonstrates how to generate probability distribution functions for regional climate, to analyse the risk of climate change on wheat production in 2080 at Roseworthy, South Australia. PDFs for regional climate change were produced through identification, quantification and treatment of uncertainties associated with projection of GHG emissions, GHG and aerosol forcing, climate sensitivity, and differences among climate models for global warming and local climate change by applying MCRS techniques. The reliability of this system was assessed within the uncertainty range quantified through cost–benefit analysis. The main advantage of this methodology is that probability can be attached to regional climate change, thus facilitating policy making decisions.

The resulting PDFs were then applied to a wheat production system represented by the APSIM-Wheat model, to examine the potential impacts of climate change on the viability of wheat production in Roseworthy, South Australia. Economic analysis shows that risks to wheat production in this area are likely to increase by 2080, with a conditional median probability of 45%. Although risk levels may decrease somewhat under some climate change scenarios, the probability of this is very low. Overall, according to these simulations, wheat production in this area is likely to become less profitable, so that adaptation strategies should be evaluated and implemented.

This study has improved upon an earlier analysis by Jones (2000b). More sources of uncertainties were incorporated into the construction of the climate change PDFs, and relationships between different uncertainty

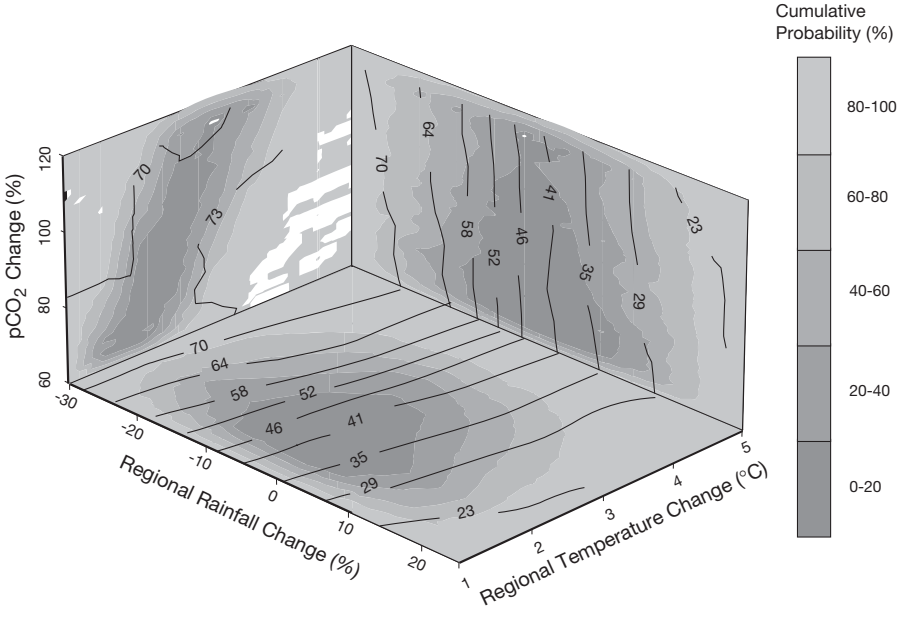


Fig. 5. Conditional probability of not exceeding the critical yield threshold in 80 future climate change scenarios at Roseworthy, South Australia, in 2080

components were incorporated and applied to MCRS techniques to constrain the distribution of the dependent components. For example, the relationship between atmospheric $pCO_2$ and regional temperature change was considered through the link of GHG and aerosol forcing. As a result, there are some blank areas in Figs. 4 & 5, indicating the impossible combination of high global warming and low atmospheric $pCO_2$.

However, these probabilities are conditional upon the input assumptions used to sample climate change uncertainties. New studies are emerging that apply probability distribution functions to climate sensitivity (summarised in Dessai & Hulme 2004, Murphy et al. 2004), regional climate change (Giorgi & Mearns 2003, Tebaldi et al. 2004) and global warming (Wigley & Raper 2001, Webster et al. 2003). Changing the methodology of Monte Carlo sampling according to a range of PDFs will alter the probabilities of threshold exceedance, but to date little work has been undertaken to investigate the effect of different prior assumptions on impacts. Jones & Page (2001) assessed different prior assumptions of likelihood and sampling methods on water resource impacts for a single catchment, deciding that the overall conclusions were little altered by the application of different strategies, although an uncertainty analysis helped explain why this was so. Jones (2004) shows that different PDFs for climate sensitivity have a significant impact on global warming at stabilisation. Weighting of model performance on regional rainfall as described by Tebaldi et al. (2004) may have a significant impact on the results. For example, the wettest model, GFDL-R15a, has the poorest performance in the region (McInnes et al. 2002). If the distribution of regional rainfall change is modified to account for model performance in simulating current climate, then the distribution becomes drier, resulting in lower yields and greater production risks.

Uncertainties also exist with regard to crop modelling. Even though the APSIM-Wheat model is a state-of-the-art crop model that performed reasonably well here, Howden & Jones (2001), using another wheat module of the APSIM system, found that climate change would increase wheat yield. Intermodel comparisons may be required to evaluate model performance and thus determine which one generates the most realistic simulations under climate change. Furthermore, the possible effects of pests, diseases and weeds on wheat production were not incorporated into the study. Future research needs include improvement of crop models, sensitivity testing of crop model with regard to climate change, and quantification of physiological effects of $CO_2$. Higher risk to wheat production was projected for Roseworthy, but this study did not consider adaptive management options to counteract the projected negative impact. These also require further investigation.

*Acknowledgements*. We thank Dr. G. Glonek (University of Adelaide) for help with Monte Carlo random sampling techniques under an S-Plus environment, Dr. I. Cooper (University of Adelaide) for providing an Excel spreadsheet for calculating the critical yield threshold, and the Australian Research Council for financial support via an ARC Linkage Grant.

## LITERATURE CITED

Ahmad QK, Warrick RA, Downing TE, Nishioka S and 5 others (2001) Methods and tools. In: McCarthy JJ, Canziani OF, Leary NA, Dokken DJ, White KS (eds) Climate change 2001: impacts, adaptation, and vulnerability. Contribution of Working Group II to the Third Assessment Report of the Intergovernmental Panel on Climate Change. Cambridge University Press, Cambridge, p 105–143

Brasseur G, Orlando J, Tyndall G (1999) Atmospheric chemistry and global change. Oxford University Press, Oxford

CSIRO (1996) Climate change scenarios for the Australian region. Climate Impact Group, CSIRO Division of Atmospheric Research, Melbourne

CSIRO (2001) Climate change projections for the Australian region. Climate Impact Group, CSIRO Division of Atmospheric Research, Melbourne

Cubasch U, Meehl GA, Boer GJ, Stouffer RJ and 5 others (2001) Projections of future climate change. In: Houghton JT, Ding Y, Griggs DJ, Noguer M, van der Linden PJ, Dai X, Maskell K, Johnson CA (eds) Climate change 2001: the scientific basis. Contribution of Working Group I to the Third Assessment Report of the Intergovernmental Panel on Climate Change. Cambridge University Press, Cambridge, p 525–582

Dessai S, Hulme M (2004) Does climate adaptation policy need probabilities? Clim Policy 4:107–128

Giorgi F, Mearns LO (2003) Probability of regional climate change based on the reliability ensemble averaging (REA) method. Geophys Res Lett 30: article no. 1629

Hansen JE, Sato M, Lacis A, Ruedy R, Tegen E, Matthews E (1998) Climate forcings in the industrial era. Proc Natl Acad Sci USA 95:12753–12758

Henderson-Sellers A (1993) An antipodean climate of uncertainty. Clim Change 25:203–224

Howden SM, Jones RN (2001) Cost and benefits of $CO_2$ increase and climate change on the Australian wheat industry. Australian Greenhouse Office, Canberra; available at www.greenhouse.gov.au/science/wheat/index.html

Howden SM, Reyenga PJ, Meinke H (1999a) Global change impacts on Australian wheat cropping. Report to the Australian Greenhouse Office, CSIRO Sustainable Ecosystems, Canberra

Hulme M, Brown O (1998) Portraying climate scenario uncertainties in relation to tolerable regional climate change. Clim Res 10:1–14

Hulme M, Carter TR (1999) Representing uncertainty in climate change scenarios and impacts studies. In: Carter TR, Hulme M, Viner D (eds) Representing uncertainty in climate change scenarios and impacts studies. Proc ECLAT-2 Helsinki Workshop, 14–16 April, 1999. Climatic Research Unit, Norwich, p 11–37

IPCC (1996) Technical summary. In: Houghton JT, Meria Filho LG, Callander BA, Harris N, Kattnberg A, Maskell K (eds) Climate change 1995: the science of climate change. Contribution of Working Group I to the Second Assessment Report of the Intergovernmental Panel on Climate Change. Cambridge University Press, Cambridge, p 9–49

Jones RN (2000a) Managing uncertainty in climate change projections—issues for impact assessment. Clim Change 45:403–419

Jones RN (2000b) Analysing the risk of climate change using an irrigation demand model. Clim Res 14:89–100

Jones RN (2001) An environmental risk assessment/management framework for climate change impact assessment. Nat Hazards 23:197–230

Jones RN, Hennessy KJ (2000) Climate change impacts in the Hunter Valley: a risk assessment of heat stress affecting dairy cattle. CSIRO Atmospheric Research, Melbourne; available at: www.dar.csiro.au/publications/Jones_2000a.pdf

Jones RN, Page CM (2001) Assessing the risk of climate change on the water resources of the Macquarie River catchment. In: Ghassemi F, Whetton P, Little R, Littleboy M (eds) Integrating models for natural resources management across disciplines, issues and scales (Part 2). MODSIM 2001, Int Congr Modelling Simulation. Modelling and Simulation Society of Australia and New Zealand, Canberra, p 673–678

Keating BA, Carberry PS, Hammer GL, Probert ME and 19 others (2003) An overview of APSIM, a model designed for farming systems simulation. Eur J Agron 18:267–288

Leavesley GH (1994) Modelling the effects of climate change on water resource—a review. Clim Change 28:159–177

Luo QY (2003) Assessment of the potential impacts of climate change on South Australian wheat production. PhD thesis, University of Adelaide

McInnes KL, Suppiah R, Whetton PH, Hennessy KJ, Jones RN (2002) Climate change in South Australia. Report on assessment of climate change, impacts and possible adaptation strategies relevant to South Australia. CSIRO Atmospheric Research, Melbourne; available at: www.environment.sa.gov.au/sustainability/pdfs/csiro_report.pdf

Mearns LO, Hulme M, Carter TR, Leemans R, Lal M, Whetton P (2001) Climate scenario development. In: Houghton JT, Ding Y, Griggs DJ, Noguer M, van der Linden PJ, Dai X, Maskell K, Johnson CA (eds) Climate change 2001: the scientific basis. Contribution of Working Group I to the Third Assessment Report of the Intergovernmental Panel on Climate Change. Cambridge University Press, Cambridge, p 739–768

Murphy JM, Sexton DMH, Barnett DN, Jones GS, Webb MJ, Collins M (2004) Quantification of modelling uncertainties in a large ensemble of climate change simulations. Nature 430:768–772

Nakiçenovic N, Davidson O, Davis G, Grübler A and 11 others (2000) The special report on emission scenarios: executive summary. Intergovernmental Panel on Climate Change, Geneva

Page CM, Jones RN (2001) OzClim: the development of a climate scenario generator for Australia. In: Ghassemi F, Whetton P, Little R, Littleboy M (eds) Integrating models for natural resources management across disciplines, issues and scales (Part 2). MODSIM 2001, Int Congr Modelling Simulation. Modelling and Simulation Society of Australia and New Zealand, Canberra, p 667–672

Parry ML, Carter TR, Hulme M (1996) What is a dangerous climate change? Global Environ Change 6:1–6

Pepper WJ, Leggett J, Swart R, Wasson J, Edmonds J, Mintzer I (1992) Emission scenarios for the IPCC. An update: assumptions, methodology, and results. In: Houghton JT, Callander BA, Varney SK (eds) Climate change 1992: supplementary report to the IPCC scientific assessment. Cambridge University Press, Cambridge

Prentice IC, Farquhar GD, Fasham MJR, Goulden ML and 6 others (2001) The carbon cycle and atmospheric carbon dioxide. In: Houghton JT, Ding Y, Griggs DJ, Noguer M, van der Linden PJ, Dai X, Maskell K, Johnson CA (eds) Climate change 2001: the scientific basis. Contribution of Working Group I to the Third Assessment Report of the Intergovernmental Panel on Climate Change. Cambridge University Press, Cambridge, p 183–237

Schneider SH (2001) What is 'dangerous' climate change? Nature 411:17–19

Tebaldi C, Mearns LO, Nychka D, Smith RL (2004) Regional probabilities of precipitation change: a Bayesian analysis of multimodel simulations. Geophys Res Lett 31: article no. L24213

Titus JG, Narayan V (1996) The risk of sea level rise. Clim Change 33:151–212

Webster M, Forest C, Reilly J, Babiker M and 7 others (2003) Uncertainty analysis of climate change and policy response. Clim Change 61:295–320

Wigley T (2003) MAGICC/SCENGEN 4.1: technical manual. National Center for Atmospheric Research, Boulder, CO

Wigley TML, Raper SCB (2001) Interpretation of high projections for global mean warming. Science 293: 451–454

Yohe GW, Schlesinger ME (1998) Sea-level change: the expected economic cost of protection or abandonment in the United States. Clim Change 38:447–472

Yunusa IAM, Bellotti WD, Moore AD, Probert ME, Baldock JA (2004) An exploratory evaluation of APSIM to simulate growth and yield processes for winter cereals in rotation systems in South Australia. Aust J Exp Agric 44:787–800

*Editorial responsibility: Otto Kinne, Oldendorf/Luhe, Germany*

*Submitted: July 16, 2004; Accepted: April 19, 2005*
*Proofs received from author(s): May 19, 2005*